doi: 10.12029/gc20200205

艾江,吕新彪,李作武,吴亚伦. 2020. 黄羊山石墨矿床地质特征及成岩年代研究[J]. 中国地质, 47(2): 334−347.
Ai Jiang, Lü Xinbiao, Li Zuowu, Wu Yalun. 2020. Geological characteristics and diagenetic geochronology of the Huangyangshan graphite deposit[J]. Geology in China, 47(2): 334−347(in Chinese with English abstract).

黄羊山石墨矿床地质特征及成岩年代研究

艾江[1],吕新彪[1],李作武[2],吴亚伦[2]
(1. 中国地质大学,湖北 武汉 430074;2. 中国建筑材料工业地质勘查中心新疆总队,新疆 乌鲁木齐 830092)

提要:黄羊山矿床是最近在新疆发现的一个超大型晶质石墨矿床,预测晶质石墨矿物量至少为72.64 Mt。该矿床赋存于花岗岩内,90%的石墨呈球粒状构造,球粒直径最高达20 cm,世界罕见。通过钻孔岩芯编录、探槽编录、镜下观察和锆石U−Pb定年,研究了该矿床矿化情况、矿物组合和成岩年代,探讨了矿床成因。研究表明,黄羊山石墨矿床成岩于(306±4)Ma,属晚石炭世。石墨球粒和基质的岩性相同,皆为碱长花岗岩,只是石墨球粒内较为富集黑云母、角闪石和单斜辉石。与石墨伴生的金属矿物主要为磁黄铁矿、黄铜矿、钛铁矿和赤铁矿。由于石墨的强还原性,这些金属矿物多分布于石墨球粒内,形成典型的环带结构。石墨矿化可分为岩浆热液期和热液叠加期2期,前者是主成矿期,形成球粒状和浸染状构造石墨,后者形成脉状构造石墨。石墨晶体呈片状和胶状结构,片状石墨横截面呈针状,定向性明显。石墨矿石的全岩碳同位素呈负低值,表明构成石墨的碳来自地层有机物。岩浆在上侵过程中同化混染了地层有机物,在岩浆演化晚期熔体相与流体相分离时,碳质溶入流体相中,当温度和压力降低时石墨从岩浆热液中沉淀成矿。中粒钠铁闪石花岗岩、细粒黑云母花岗岩和中粒黑云母花岗岩中皆含石墨球粒,黄羊山岩体仍具有巨大找矿潜力。

关 键 词:石墨矿床;矿床地质;矿床成因;锆石U−Pb定年;地质调查工程;黄羊山;新疆
中图分类号:P597.3;P612 **文献标志码**:A **文章编号**:1000−3657(2020)02−0334−14

Geological characteristics and diagenetic geochronology of the Huangyangshan graphite deposit, Xinjiang

AI Jiang[1], LÜ Xinbiao[1], LI Zuowu[2], WU Yalun[2]
(1. *China University of Geosciences, Wuhan* 430074*, Hubei, China;* 2. *Xinjiang General Party, China National Geological Exploration Center of Building Materials Industry, Urumqi* 830092*, Xinjiang, China*)

Abstract: The Huangyangshan deposit is a superlarge crystalline graphite deposit recently discovered in Xinjiang. The reserves of crystalline graphite in the deposit are estimated at least 72.64 Mt. The deposit is hosted in granite, and 90% of graphite is of spherulitic structure. The longest diameter of the spherulite can reach 20 cm. It is extremely rare in the world. Through drill core logging, prospecting trench logging and petrographic and zircon U− Pb geochronologic studies, the authors investigated

收稿日期:2018−03−05;**改回日期**:2019−09−22
基金项目:中国地质调查局项目"新疆奇台县黄羊山一带石墨矿调查评价"(DD20160058−01)资助。
作者简介:艾江,男,1988年生,博士生,矿产普查与勘探专业;E−mail: jiangai@cug.edu.cn。
通讯作者:吕新彪,男,1962年生,教授,博士生导师,矿床学与矿产资源预测评价;E−mail: Lvxb_01@163.com。

mineralization, mineral assemblage and diagenetic age of the deposit, and discussed its ore genesis. The results reveal that the diagenetic age of the deposit is (306±4) Ma, which is Late Carboniferous. Graphite spherulite and matrix have the same lithology of alkali−feldspar granite. However, biotite, hornblende and clinopyroxene are relatively more concentrated in the spherulite. Metallic minerals associated with graphite are pyrrhotite, chalcopyrite, ilmenite and hematite. Due to strong reducibility of graphite, these metallic minerals are mainly distributed within graphite spherulite, forming typical zoning texture. Graphitization could be divided into two periods, namely magmatic hydrothermal period and hydrothermal superimposition period. The former was the principal ore-forming period, producing spherulitic and disseminated graphite, while the latter produced vein graphite. Crystals of graphite are of flaky and colloform texture. The flaky graphite is in acicular form along the section and has preferred orientations. Graphite ores have low negative bulk−rock carbon isotopic composition, which implies that the carbon consisting of graphite was derived from organic matters in strata. Magma assimilated organic matters in strata during its ascending. At the late stage of magma evolution, with the separation of the melt and liquid phase, carbonaceous matters were incorporated into the liquid phase. When the temperature and pressure decreased, carbon precipitated from the magmatic hydrothermal to form graphite. Medium- grained arfvedsonite granite and fine and medium grained biotite granite contain graphite spherulites, and hence Huangyangshan pluton has considerable ore−prospecting potential.

Key words: graphite deposit; deposit geology; ore genesis; zircon U− Pb geochronology; geological survey engineering; Huangyangshan; Xinjiang

About the first author: AI Jiang, male, born in 1988, doctor candidate, majors in mineral prospecting and exploration; E−mail: jiangai@cug.edu.cn.

About the corresponding author: LÜ Xinbiao, male, born in 1962, professor, supervisor of doctor candidates, mainly engages in research on mineral deposits and prediction and evaluation of mineral resources; E−mail: Lvxb_01@163.com.

Fund support: Supported by the project of “Investigation and evaluation of graphite ore in Huangyangshan area, Qitai County, Xinjiang” from China Geological Survey (No. DD20160058−01).

1 引 言

石墨的化学式为C，具有优越的电、热绝缘性和柔软性，其常被用来生产高科技产品，如石墨烯、电动汽车、润滑剂、燃料电池、半导体和锂离子电池（Rosing−Schow et al., 2017）。全球对石墨的需求正呈逐年增长之势（Hao et al., 2016）。因此，石墨已被很多国家定为战略矿产资源（Luque et al., 2014）。中国是生产和出口石墨的大国，每年石墨产量和出口量占全球70%以上（姜高珍,2016）。2016年，中国成为了全球第三大石墨出口国，出口量约为55 Mt（Jewell and Kimball, 2017）。石墨通常由碳质富集沉淀或变质形成，前者通常形成块状（粗粒晶质）石墨（C含量高达99%），后者往往形成非晶质（隐晶质）和片状（晶质）石墨（C含量高达75%~97%）（Crespo et al.,2004; Luque et al., 2012）。石墨的沉淀由三个因素决定：（1）含碳载体成分发生变化，如流体与无水矿物在围岩中发生水合反应，或有不同CO_2/CH_4比值的流体混合；（2）温度降低；（3）还原反应（Rumble, 2014）。石墨可通过5种反应沉淀：（1）$CH_4 \rightarrow C+2H_2$；（2）$CO_2 \rightarrow C+O_2$；（3）$CH_4+CO_2 \rightarrow 2C+2H_2O$；（4）$CH_4+O_2 \rightarrow C+2H_2O$；（5）$CO_2+2H_2 \rightarrow C+2H_2O$（Ortega et al., 2010）。这些反应所需的温度范围为100~1000℃，压力大于2×10^5 kPa（Luque et al., 1998; Huizenga, 2011）。石墨有3种碳质来源：地幔碳、地层无机碳和地层有机碳。地幔碳主要以CO_2形式被岩浆从地幔运移至地壳，岩浆发生分离结晶，富CO_2流体与岩浆分离，经过水合反应、冷却或还原反应，石墨从流体中沉淀析出。地层无机碳可通过脱碳反应（如$6FeCO_3 \rightarrow 2Fe_3O_4+CO_2+C$），同样经过水合反应、冷却和还原反应沉淀石墨（Zuilen et al., 2003）。地层有机碳可被岩浆同化混染，岩浆分离结晶时富碳残余熔浆和C−O−H流体发生分离。富碳残余岩浆冷却时石墨从岩浆中沉淀析出形成岩浆型石墨，而C−O−H流体可运移至岩浆顶部、边部或外部沉淀石墨形成热液型石墨（Luque et al., 2014）。

新疆昌吉州奇台县境内黄羊山地区是新疆最大的石材生产基地，自20世纪80年代在黄羊山岩体内发现中型规模的苏吉泉石墨矿床后，前人前赴后继，终于在近年来取得了重大找矿成果。2015年

黄羊山石墨矿床被发现,经过近3年的勘查工作,共圈定8个晶质石墨矿体,探明晶质石墨矿物量达超大型规模。通常晶质石墨矿物资源量达到1 Mt即定为大型矿床,而黄羊山矿床仅1号和2号矿体的晶质石墨矿物资源量就达到了72.64 Mt,可将其定为超大型矿床。石墨矿床多赋存于变质岩中,而赋存于侵入岩中且达超大型规模的石墨矿床屈指可数,全球已知的主要有Serrania de Ronda(西班牙)、Beni Bousera(摩洛哥)、Botogol和Pogranichnoe(俄国)(Luque et al., 2014)。这些矿床的赋矿围岩主要为基性、超基性岩,而像黄羊山一样赋存于酸性岩中且资源量达超大型规模的石墨矿床尚未有任何报道。况且,国外矿床中石墨球粒少而小,直径不超过5 cm,而黄羊山矿床中90%的石墨呈球粒状构造产出,直径长达20 cm。因此,黄羊山矿床是世界罕见的石墨矿床,具有重大研究和经济价值,应当倍受关注。但是,目前该矿床成因尚未研究清楚,影响矿区及外围进一步找矿工作。深入研究黄羊山矿床的成矿地质条件、矿石特征和成矿年代学特征,探讨其成因及成矿规律,对在该地区厘定找矿方向且在其他地区寻找和评价此类矿床具有重要意义,也可为完善碳在侵入岩中迁移、富集和沉淀形成球粒状石墨成矿机制提供理论依据。本文通过详细的野外地质考察、岩相学观察和锆石U-Pb定年,对该矿床地质特征及成岩年代进行了研究,初步探讨该矿床成因。

2 区域地质背景

东准噶尔造山带处于天山造山带和阿尔泰造山带之间,西缘为准噶尔盆地。东准噶尔造山带自北向南分别由杜拉特岛弧带、阿尔曼太蛇绿岩带、野马泉岛弧带、卡拉麦里蛇绿岩带和哈尔里克地块六部分组成(图1a; 宋利宏等,2015)。黄羊山石墨矿床位于新疆昌吉州奇台县北西约160 km的黄羊山岩体内,有高速公路从矿区经过,交通方便。在大地构造上,该矿床位于东准噶尔造山带南缘卡拉麦里缝合带以北的野马泉岛弧带内(图1a),清水—苏吉泉断裂为卡拉麦里缝合带与野马泉岛弧带的界线(图1b)。

区域内出露的地层从老到新主要包括古生界、中生界和新生界,其中古生界出露面积较大,由奥陶系、志留系、泥盆系、石炭系和二叠系为主(赵磊等,2019)。奥陶系岩性主要为火山角砾岩、凝灰岩、安山岩、砂岩、片岩等。志留系岩性主要为火山碎屑岩夹碳酸盐岩。泥盆系岩性主要为中性-中基性火山岩、火山碎屑岩、碳酸盐岩等。石炭系岩性主要为陆源碎屑岩及火山碎屑岩建造。二叠系岩性主要为杂色陆相陆源碎屑岩夹泥灰岩、陆相双峰式火山岩建造和红色磨拉石沉积建造(刘光海等,1995)。区域内深大断裂主要有两条,分别为限定卡拉麦里缝合带北部和南部边界的清水—苏吉泉断裂和卡拉麦里断裂,其中清水—苏吉泉断裂为花岗岩类侵入野马泉岛弧带提供了运移通道(黄岗等,2017),也为区内金矿床的形成提供了沉淀场所(高怀忠等,2000; 张栋等,2011; 张玉杰等,2013)。这些花岗岩类侵入于华力西晚期,以岩基或岩株形式产出,以偏碱性花岗岩为主,具有代表性的岩体由北至南分别为野马泉、老鸭泉、贝勒库都克和黄羊山(图1b)。

3 矿床地质特征

3.1 矿区地质

矿区内出露的地层主要为下石炭统黑山头组和姜巴斯套组,二者皆为火山-沉积岩(杨高学,2009b)。矿区内出露的侵入岩主要为中泥盆世斜长花岗岩(聂晓勇等,2016)和晚石炭世碱长花岗岩(Yang et al., 2011),后者被称为黄羊山岩体。按照所含暗色矿物组成和矿物粒径的变化,该岩体被划分为六种岩相,即由北向南依次为细粒钠铁闪石花岗岩、中粒钠铁闪石花岗岩、角闪石花岗岩、含石墨花岗岩、细粒黑云母花岗岩和中粒黑云母花岗岩,其中含石墨花岗岩即为石墨矿石(图2)。原先黄羊山岩体只包括位于中部的中粒钠铁闪石花岗岩和角闪石花岗岩两个岩相,而位于北部的细粒钠铁闪石花岗岩属于萨北岩体,位于南部的含石墨花岗岩、细粒黑云母花岗岩和中粒黑云母花岗岩属于苏吉泉岩体(毕承思等,1993; 刘家远等,1997,1998,1999; 吴郭泉等,1997; 喻亨祥等,1998; 苏玉平等,2006; 林锦富等,2007; 唐红峰等,2007; 刘松柏等,2011)。经过岩相学和地球化学研究,杨高学等(2009a,2010)将萨北岩体和苏吉泉岩体划归黄羊山岩体。

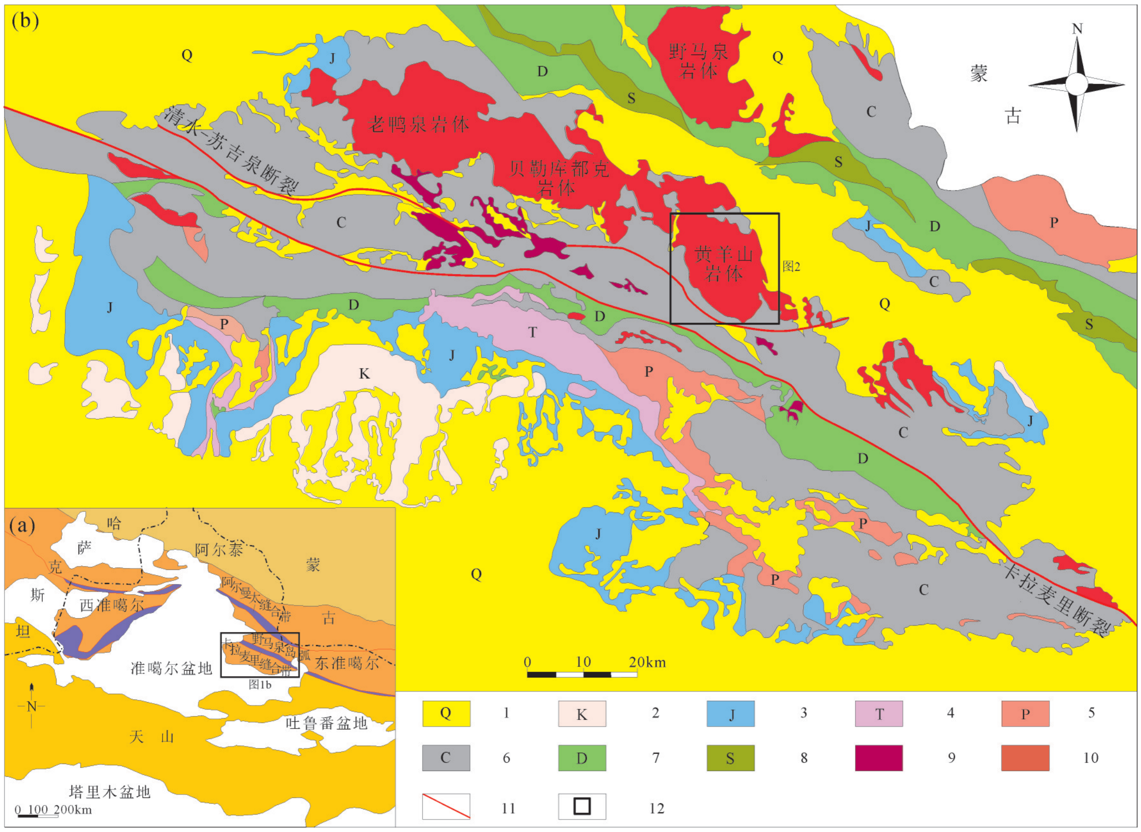

图1 新疆东准噶尔造山带地质简图(据宋利宏等,2015)
1—第四系;2—白垩系;3—侏罗系;4—三叠系;5—二叠系;6—石炭系;7—泥盆系;8—志留系;9—蛇绿岩;
10—花岗岩类;11—断裂;12—研究区
Fig.1 Geological map of East Junggar orogenic belt, Xinjiang (modified from Song Lihong et al., 2015)
1-Quaternary; 2-Cretaceous; 3-Jurassic; 4-Triassic; 5-Permian; 6-Carboniferous ; 7-Devonian; 8-Silurian; 9-Ophiolite;
10-Granitoids; 11-Fault; 12-Research area

秦学庆和刘远珍(1986)、莫如爵等(1989)、严正富等(1990)、张国新等(1996)、唐延龄等(2005)、杨宝凯等(2010)和刘松柏等(2011)将沿着角闪石花岗岩和细粒黑云母花岗岩接触带分布的含石墨花岗岩命名为“混染花岗岩”,其是苏吉泉石墨矿床的赋矿岩石。“混染作用”是岩浆演化过程中普遍存在的一种地质现象,多数侵入岩在形成过程中都会经历混染作用,几乎所有花岗岩都可以称为“混染花岗岩”,因此本文认为“混染花岗岩”这种命名无法准确反映石墨矿石的岩性特征。新疆建材勘查总队在2015年苏吉泉石墨矿床外围开展的找矿工作中取得了重大进展,发现了以隐伏于角闪石花岗岩中的石墨矿体为主的超大型石墨矿床,并将其命名为黄羊山石墨矿床(张小林等,2017; Ai et al., 2018)。苏吉泉和黄羊山两个石墨矿床的矿体形态和位置如图2所示。

本次野外实地考察时,笔者在中粒钠铁闪石碱长花岗岩、细粒黑云母碱长花岗岩和中粒黑云母碱长花岗岩中都发现了零星孤立分布、直径为6~7 cm的石墨球粒,说明组成黄羊山岩体的各个期次花岗岩都是含石墨的,只是石墨的含量和分布不均匀罢了。

3.2 矿体特征

黄羊山石墨矿床由8个矿体组成,其中1号和2号矿体赋存于角闪石碱长花岗岩中,3号和4号矿体赋存于细粒黑云母碱长花岗岩中,5号至8号矿体赋存于中粒黑云母碱长花岗岩中(图2)。1号矿体为隐伏矿体,呈透镜状产出,长2100 m,宽250~730 m,埋深为125~481 m,平均厚度310 m,品位为6.14%,片径为0.15 mm的石墨平均含量约为10%,晶质石墨矿物资源量为4740 Mt(张小林等,2017; Ai et al.,

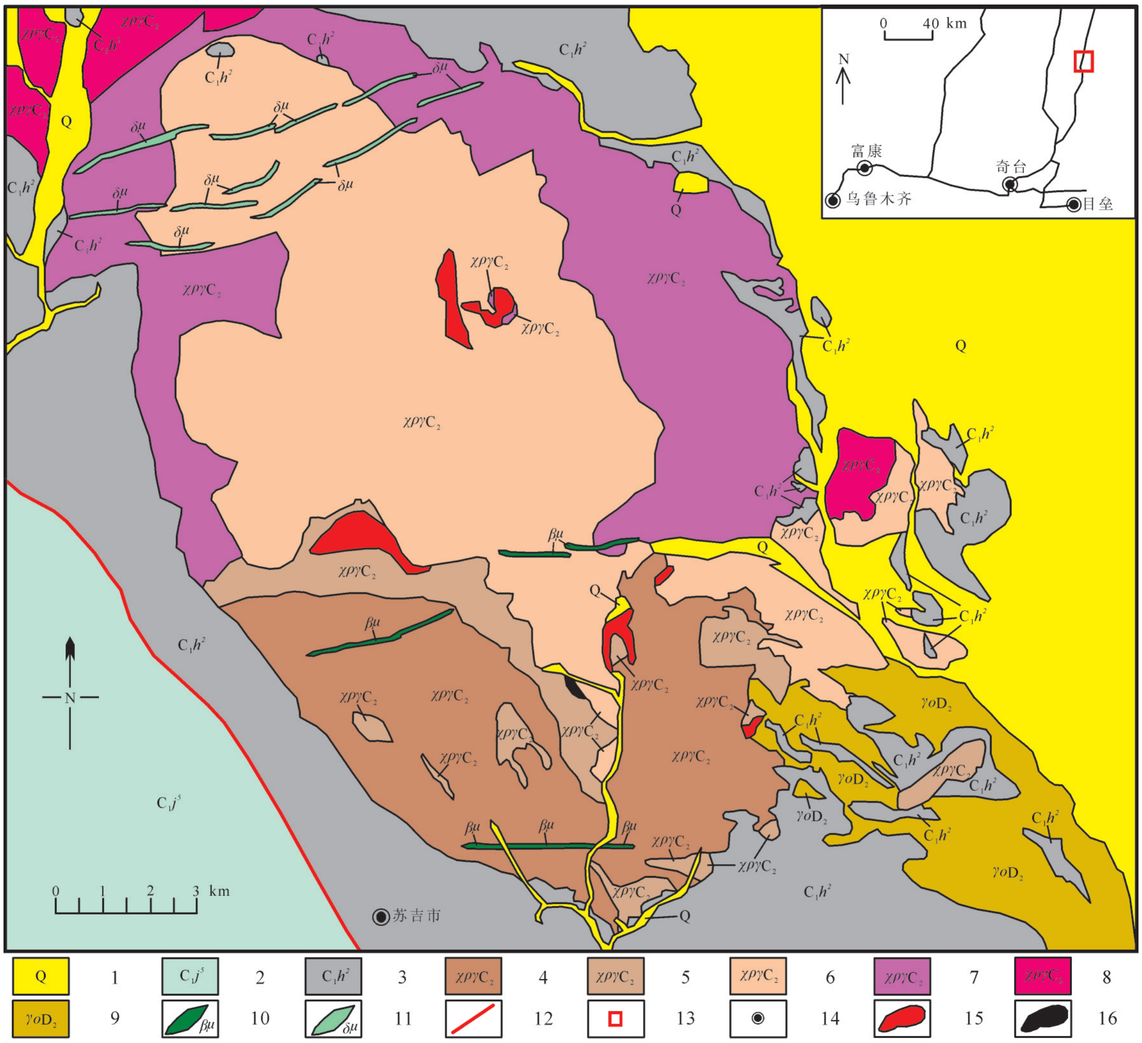

图2 新疆东准噶尔黄羊山地区地质图(据张小林等,2017修改)

1—第四系;2—下石炭统姜巴斯套组;3—下石炭统黑山头组;4—晚石炭世中粒黑云母碱长花岗岩;5—晚石炭世细粒黑云母碱长花岗岩;6—晚石炭世角闪石碱长花岗岩;7—晚石炭世中粒钠铁闪石碱长花岗岩;8—晚石炭世细粒钠铁闪石碱长花岗岩;9—中泥盆世斜长花岗岩;10—辉绿(玢)岩脉;11—闪长(玢)岩脉;12—清水—苏吉泉断裂;13—研究区;14—城镇;15—黄羊山石墨矿床矿体;16—苏吉泉石墨矿床矿体

Fig. 2 Geological map of Huangyangshan area, Xinjiang (modified from Zhang Xiaolin et al., 2017)

1−Quaternary; 2−Lower Carboniferous Jiangbasitao Formation; 3−Lower Carboniferous Heishantou Formation; 4−Late Carboniferous medium grained biotite alkali−feldspar granite; 5−Late Carboniferous medium-grained biotite alkali−feldspar granite; 6−Late Carboniferous hornblende alkali−feldspar granite; 7−Late Carboniferous medium-grained arfvedsonite alkali−feldspar granite; 8−Late Carboniferous fine-grained arfvedsonite alkali−feldspar granite; 9−Middle Devonian plagioclase granite; 10−Diabase vein; 11−Diorite vein; 12−Qingshui−Sujiquan fault; 13−Research area; 14−Town; 15−Orebodies of Huangyangshan graphite deposit; 16−Orebodies of the Sujiquan graphite deposit

2018)。2号矿体出露于地表,呈柱状产出,长1100 m,宽200~580 m,埋深为383.2 m,品位为7.04%,片径为0.15 mm的石墨平均含量约为30%~35%,晶质石墨矿物资源量约为2560 Mt(张小林等,2017; Ai et al., 2018)。该两个矿体倾向南西,其顶板围岩为角闪石碱长花岗岩,底板围岩为细粒黑云母碱长花岗岩,矿体与围岩的界线截然。在顶底板围岩内与矿体接触的部位,石墨多呈浸染状产出(图3a),偶见含石墨的暗绿色包体(图3b),此类包体与矿体的岩性较为相似,说明矿体上侵时与围岩发生了混染。矿体中石墨主要呈球粒状构造,少量呈浸染状和细脉状构造(图3c−f)。

3.3 矿石特征

矿石岩性为含石墨碱长花岗岩,含约70%碱性长石、5%斜长石、25%石英及<1%的角闪石和单斜辉石。碱性长石以条纹长石和钾长石形式产出。

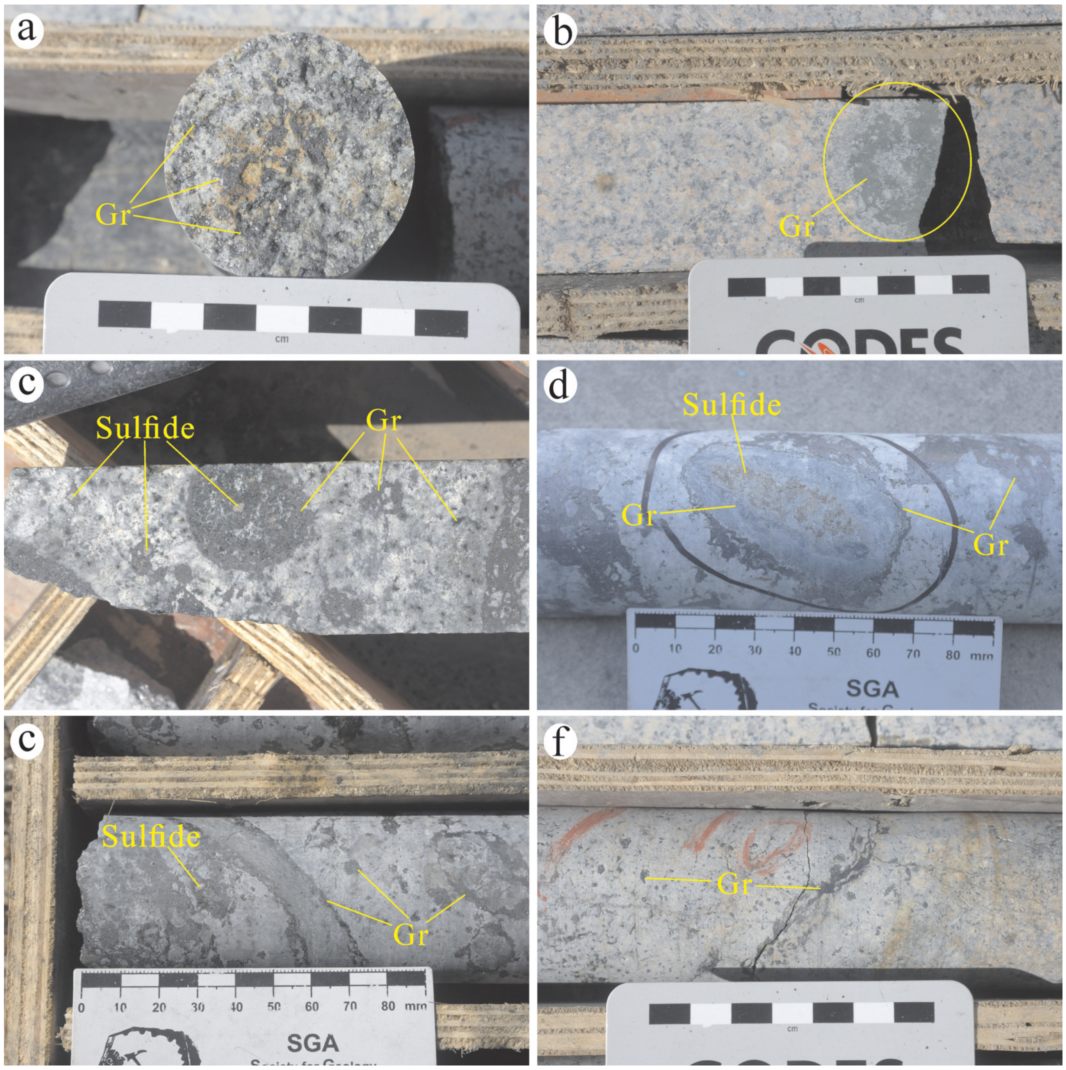

图3 黄羊山石墨矿床矿石构造

a—角闪石花岗岩中浸染状石墨;b—角闪石花岗岩中石墨矿石包体;c—矿石中球粒状和浸染状石墨;d—矿石中具有环带结构的石墨球粒;e、f—矿石中细脉状和浸染状石墨;Gr—石墨;Sulfide—硫化物

Fig.3 Structures of ores in the Huangyangshan graphite deposit

a−Disseminated graphite in hornblende granite; b−Xenoliths of graphite ores in hornblende granite; c−Spherulitic and disseminated graphite in ores; d−Graphite spherulite with zoning texture in ores; e, f−Veinlet and disseminated graphite in ores; Gr−graphite; Sulfide−Sulfide

条纹长石通常为钠长石条纹出溶在钾长石主晶内。对位于1号矿体的ZK901钻孔从上到下按一定间隔采集的共7件样品进行镜下石墨球粒内外主要造岩矿物的含量和种类统计,结果如表1所示。将其投于QAP图,它们都落在碱长花岗岩区域内(图4),说明石墨球粒内外岩性相同。但是,造岩矿物含量稍有不同,如斜长石和石英在石墨球粒内相对较多,而碱性长石在基质内较多。此外,暗色矿物如角闪石和单斜辉石也在石墨球粒内较为富集。单斜辉石边缘多被角闪石交代,形成反应边结构。

表1 黄羊山石墨矿床ZK901钻孔石墨矿石岩石学特征

Table 1 Petrologic characteristics of graphite ores in drill core ZK901 in the Huangyangshan graphite deposit

主要矿物含量/%	碱性长石	斜长石	石英
石墨球粒内	60~70	5~10	25~30
基质	70~80	5~10	20~25

石墨晶体通常呈片状和胶状结构。片状石墨为结晶度较好的单个石墨晶体,其横截面呈针状,定向排列非常明显(图5a、b)。胶状石墨为隐晶质石墨晶体的集合体,呈不规则状,无法区分晶体边

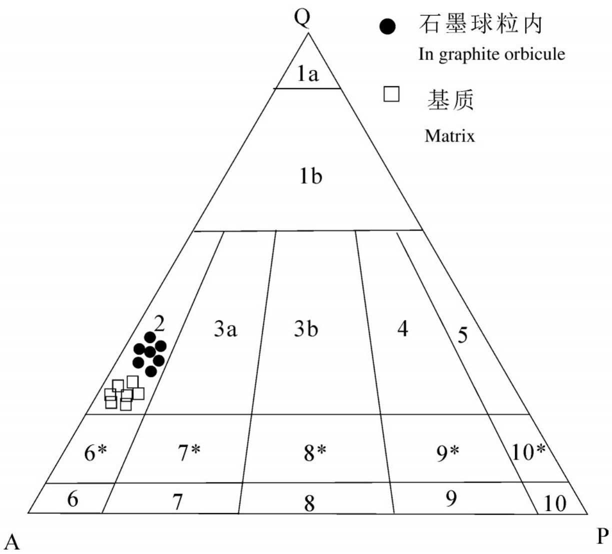

图4 花岗岩类岩石分类Q–A–P图(底图据IUGS,1972推荐)
Q—石英;A—碱性长石;P—斜长石;1a—石英岩;1b—富石英花岗岩;2—碱长花岗岩;3a—正长花岗岩;3b—二长花岗岩;4—花岗闪长岩;5—英云闪长岩;6—碱长正长岩;6*—石英碱长正长岩;7—正长岩;7*—石英正长岩;8—二长岩;8*—石英二长岩;9—二长闪长岩/二长辉长岩;9*—石英二长闪长岩/石英二长辉长岩;10—闪长岩/辉长岩/斜长岩;10*—石英闪长岩/石英辉长岩/石英斜长岩

Fig.4 Granitoids classification Q–A–P diagram (base diagram after IUGS, 1972)
Q– Quartz; A– Alkali feldspar; P– Plagioclase; 1a– Quartzite; 1b–Quartz– enriched granite; 2– Alkali– feldspar granite; 3a– Syenite granite; 3b–Monzonitic granite; 4–Granodiorite; 5–Tonalite; 6–Alkali–feldspar syenite; 6*– Quartz alkali– feldspar syenite; 7– Syenite; 7*–Quartz syenite; 8–Monzonite; 8*–Quartz monzonite; 9–Monzodiorite/Monzogabbro; 9*– Quartz monzodiorite/Quartz monzogabbro; 10–Diorite/gabbro/plagioclasite; 10*– Quartz diorite/quartz gabbro/quartz plagioclasite

界(图5c、d)。片状和胶状石墨穿插硅酸盐矿物边界,并交代硅酸盐矿物,说明石墨晚于硅酸盐矿物形成。石墨具有强还原性,因而在石墨球粒内部有大量金属矿物(磁黄铁矿、黄铜矿、钛铁矿、赤铁矿)与石墨紧密伴生,有些构成典型的环带结构:石墨位于边部,金属矿物位于核部,其间为硅酸盐矿物(图3d,图5c)。金属矿物也呈脉状产出,穿插早期形成的石墨和金属矿物(图5e、f)。矿体发生了强烈的绿泥石化和绢云母化蚀变。

3.4 矿化期次

脉状石墨穿插球粒状和浸染状石墨,说明石墨由2期成矿作用形成。第一成矿期石墨呈球粒状和浸染状构造产出,第二成矿期石墨呈脉状构造产出。其中,第一期为主成矿期。

4 锆石U–Pb定年

4.1 样品采集和分析方法

本次采集了1号矿体ZK901钻孔内1件石墨矿石样品用于锆石U–Pb定年测试。样品较为新鲜,没有经过风化和蚀变作用影响,也没有岩脉穿插,能基本代表成矿期样品。锆石挑选和制靶在中国科学院广州地球化学研究所进行。LA–ICP–MS锆石U–Pb定年测试在中国地质大学(武汉)进行。从样品中挑选出来的锆石多为长柱状,呈半自形或自形颗粒,长85~130 μm,宽20~40 μm,长宽比值为3∶1。锆石内部显现平面生长和典型的振荡环带结构,其与岩浆锆石的特征相吻合。从这些锆石中挑选出没有裂痕和包裹体的锆石作为研究对象,使用配备有Geolas 2005激光剥蚀系统的Agilent 7700a ICP–MS,将193 nm波长ArF–Excimer激光以24 μm直径光斑形式投射在20个具有振荡环带的点位(图6a),剥蚀并收集这些点位的微量元素和U–Pb同位素组成数据。每打5个点就测试一次标样91500和GJ–1,以便校正和监测测试数据。将测试数据输入8.3版本的ICPMSDataCal软件计算了同位素年龄,通过4.15版本的Isoplot软件绘制了谐和曲线图。

4.2 测试结果

测试结果列于表2,锆石的Th含量变化为108×10^{-6}~611×10^{-6},U含量变化为236×10^{-6}~708×10^{-6},Th/U比值范围为0.45~1.14,其与岩浆锆石的特征相吻合(Corfu et al., 2003)。用测试数据做成的谐合曲线图如图6b所示。$^{206}Pb/^{238}U$年龄范围为294~332 Ma,加权平均年龄为(306±4)Ma。该值应为石墨矿体的成岩年龄,但不是成矿年龄,因为岩相学特征表明石墨是在岩浆结晶后成矿的,在石墨沉淀前岩浆锆石已经形成。该年龄值与区内细粒钠铁闪石碱长花岗岩((313±2)Ma; 林锦富等,2007)、中粒钠铁闪石碱长花岗岩((314±5)Ma; 林锦富等,2007)、角闪石碱长花岗岩((311±12)Ma; Yang et al., 2011)和中粒黑云母碱长花岗岩((304±2)Ma; 苏玉平等,2006)的岩浆锆石U–Pb年龄相似,都为晚石炭世。

区内角闪石碱长花岗岩中岩浆锆石的Th含量为0.77×10^{-6}~427.1×10^{-6},U含量为2.1×10^{-6}~$647.6\times$

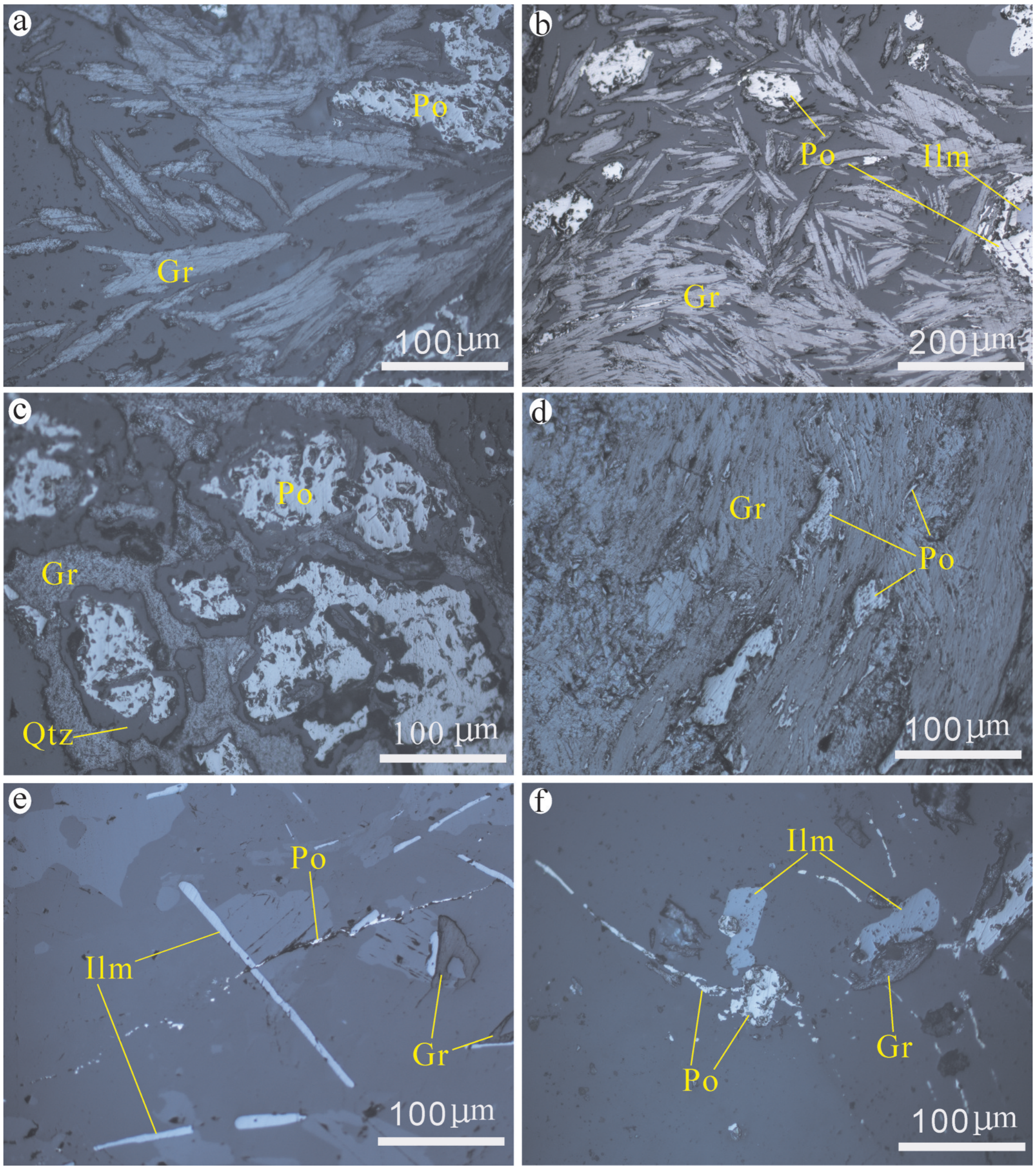

图5 黄羊山石黑矿床矿石结构

a、b—矿石中针状、束状和纤维状石墨;c—矿石中被石墨包裹的磁黄铁矿,具环带结构;d—矿石中分布于石墨晶体内的磁黄铁矿;e—矿石中分布于石黑球粒内的针状钛铁矿,其被细脉状磁黄铁矿穿插;f—矿石中石墨球粒内被细脉状磁黄铁矿穿插的不规则状磁黄铁矿;Gr—石墨;Po—磁黄铁矿;Ilm—钛铁矿;Qtz—石英

Fig. 5 Texture of ores in the Huangyangshan graphite deposit

a, b−Needle−like, bunchy and fibrous graphite in ores; c−Pyrrhotite embraced by graphite with zoning texture; d−Pyrrhotite distributed in graphite crystals; e−Needle−like ilmenite crosscut by veinlet pyrrhotite within graphite spherulite; f−Irregular pyrrhotite crosscut by veinlet pyrrhotite within graphite spherulite; Gr−Graphite; Po−Pyrrhotite; Ilm−Ilmenite; Qtz−Quartz

10^{-6}, Th/U比值范围为0.35~0.96(Yang et al., 2011)。区内细粒和中粒钠铁闪石碱长花岗岩中岩浆锆石的Th/U比值范围分别为0.34~0.71和0.20~1.05(林锦富等,2007)。将这些岩浆锆石的Th、U含量和Th/U比值与黄羊山石墨矿体中岩浆锆石的相应参数进行对比,不难看出它们的数值较为相似,说明此次从岩浆锆石中测得的同位素数据较为可靠。

5 讨　论

5.1 大地构造环境

在早古生代至晚古生代的造山作用下,东准噶

表2 黄羊山石墨矿床HYS-0001样品锆石LA-ICP-MS U-Pb定年数据
Table 2 Zircon LA-ICP-MS U-Pb geochronological data of sample HYS-0001 in the Huangyangshan graphite deposit

点号	Th/10⁻⁶	U/10⁻⁶	Th/U	$^{207}Pb/^{206}Pb$		$^{207}Pb/^{235}U$		$^{206}Pb/^{238}U$		$^{206}Pb/^{238}U$	
				比值	1σ	比值	1σ	比值	1σ	年龄/Ma	1σ
P1.1	162	265	0.61	0.0517	0.0024	0.3298	0.0155	0.0474	0.0006	298	3
P2.1	258	385	0.67	0.0529	0.0021	0.3475	0.0182	0.0486	0.0006	306	3
P3.1	153	324	0.47	0.0524	0.0026	0.3352	0.0234	0.0485	0.0006	305	3
P4.1	594	708	0.83	0.0547	0.0019	0.3474	0.0259	0.0488	0.0005	307	3
P5.1	224	397	0.56	0.0518	0.0024	0.3250	0.0311	0.0493	0.0006	310	3
P6.1	108	236	0.45	0.0518	0.0027	0.3053	0.0359	0.0470	0.0006	296	4
P7.1	611	656	0.93	0.0492	0.0020	0.2957	0.0335	0.0473	0.0005	298	3
P8.1	319	446	0.71	0.0500	0.0023	0.3148	0.0303	0.0485	0.0005	305	3
P9.1	177	287	0.61	0.0545	0.0029	0.3587	0.0297	0.0499	0.0006	314	4
P10.1	167	253	0.66	0.0507	0.0027	0.3218	0.0211	0.0470	0.0005	296	3
P11.1	221	423	0.52	0.0524	0.0031	0.3416	0.0196	0.0467	0.0005	294	3
P12.1	492	589	0.83	0.0510	0.0031	0.3502	0.0155	0.0480	0.0005	302	3
P13.1	292	304	0.96	0.0516	0.0033	0.3767	0.0173	0.0504	0.0007	317	4
P14.1	305	509	0.59	0.0516	0.0027	0.3562	0.0134	0.0479	0.0005	302	3
P15.1	368	539	0.68	0.0554	0.0028	0.4159	0.0169	0.0529	0.0007	332	4
P16.1	526	458	1.14	0.0510	0.0022	0.3695	0.0143	0.0507	0.0005	318	3
P17.1	237	320	0.74	0.0511	0.0024	0.3591	0.0164	0.0497	0.0006	313	3
P18.1	241	427	0.56	0.0524	0.0023	0.3530	0.0151	0.0482	0.0005	303	3
P19.1	169	317	0.53	0.0509	0.0025	0.3256	0.0185	0.0474	0.0006	299	4
P20.1	164	259	0.63	0.0575	0.0031	0.3543	0.0285	0.0477	0.0007	300	4

尔造山带形成“沟-弧-盆”体系(肖文交等,2006; 聂峰等,2014)。泥盆纪至早石炭世,清水—苏吉泉断裂以南形成一个次生洋盆,其向北俯冲闭合(Huang et al., 2013)。晚石炭世,东准噶尔由碰撞造山阶段进入后碰撞伸展阶段(李锦轶等,1990; 李锦轶,2004; 张栋等,2011),大量非造山型花岗岩沿着苏吉泉大断裂侵入野马泉岛弧带内黄羊山地区(刘家远等,1998; 喻亨祥等,1998)。新疆北部后碰撞成矿作用有三个高峰期,分别为340~330 Ma、300~285 Ma、270~260 Ma(王京彬等,2006)。黄羊山石墨矿床的成岩年龄值范围为294~332 Ma,加权平均值为(306±4)Ma,这一结果介于第一和第二成矿高峰期,表明该矿床为后碰撞岩浆活动的产物。

5.2 球粒状石墨成因

球粒的英文地质专业术语为orbicule、orb、globule、ocelli、rapakivi、spherulite和variole,通常指由核和壳构成的一种圆形至椭圆形地质体(Grosse et al., 2010; Ballhaus et al., 2015)。球粒核多为围岩碎块或来自侵入岩的矿物集合体,而球粒壳多为呈放射状、树枝状和同心环状的侵入岩(Elliston, 1984; Decrite et al., 2002)。球粒状构造产出于各种侵入岩(花岗岩、闪长岩、辉长岩、碳酸岩、金伯利岩、煌斑岩、正长岩等)的边缘,与结晶前沿(crystallization front)、岩浆-围岩反应区或岩浆裂隙紧密相关(Fernandez and Castro, 1999; Abdallah et al., 2007; Grosse et al., 2010; Zurevinski and Mitchell, 2015)。地质学家对球粒状构造的研究已近一个世纪,对球粒状构造的成因提出岩浆成因、变质成因和交代成因三种观点(Vernon, 1985; Meyer and Alther, 1991; Lindh and Nasstrom, 2006; Grosse et al., 2010; Ballhaus et al., 2015)。流体不混溶是一种岩浆分异作用,指一种均质岩浆分离为两种不相溶的岩浆熔体,或者分离为彼此不相溶的一种流体和一种熔体(Best, 1982; Taylor et al., 1992)。实验已证实,球粒是不相溶流体或熔体最易于形成的形状(Ballhaus et al., 2015)。过热作用(superheating)或过冷作用(undercooling)是导致流体不混溶作用发生的一种最常见的地质现象(Smillie and Turnbull, 2014; Diaz-Alvarado et al., 2017)。过热作用通常由较高温的镁铁质岩浆侵入中酸性岩浆或由含水流体涌入贫水熔体中引发,导致晶体成核速率降低而生长速率升高,继而发生过

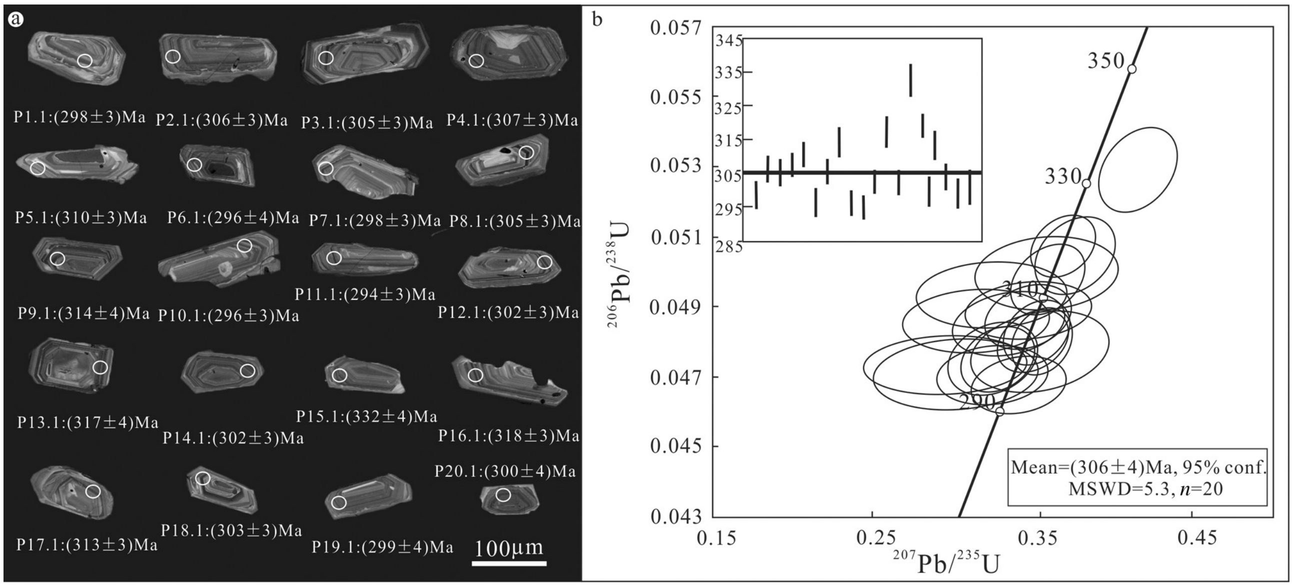

图6 黄羊山石黑矿床HYS−0001样品锆石U−Pb定年点位图(a)与年龄谐和曲线图(b)
Fig. 6 U−Pb testing spot locations in zircons (a) and concordia diagram (b) of sample HYS−0001 in the Huangyangshan graphite deposit

冷作用,岩浆的液相线温度降低,液相线以下的矿物(如角闪石)开始结晶,形成放射状和树枝状结构(Vermon, 1985)。虽然前人提出了很多假说解释该构造的成因,但是没有哪一种假说是万能的(Neef, 1991)。

在自然界中产出的球粒状石墨是非常罕见的,到目前为止报道过的只有日本音调津(Oshirabetsu)(森原望等,2012)、俄罗斯Pogranichnoe(Doroshkevich et al., 2007)和斯里兰卡Bogala(Luque et al., 2014)。前二者为岩浆成因,后者为热液成因。在中国,首个含球粒状石墨的苏吉泉矿床于20世纪80年代在黄羊山岩体中被发现,2015年在该矿床外围又发现了含球粒状石墨的黄羊山矿床(张小林等, 2017;Ai et al., 2018)。黄羊山石墨矿床与苏吉泉石墨矿床有很多相似的矿化特征,如二者都含有大量球粒状石墨,球粒内富集角闪石和黑云母,且矿体顶底板围岩中含有矿石包体等,因此本文认为黄羊山矿床与苏吉泉矿床同源、同因,二者应为同阶段演化产物。前人对苏吉泉矿床中球粒状石墨成因提出了3种假说:(1)岩浆熔体上侵过程中石墨在熔体中结晶并滚动形成球粒状(张国新等,1996; 杨宝凯等,2010;刘松伯等, 2011);(2)岩浆在上侵过程中混染花岗质围岩,围岩碎块作为球粒核,石墨在岩浆中围绕该核结晶形成球粒壳(莫如爵,1989);(3)石墨在与岩浆熔体不相溶的球形热液中沉淀形成球状构造(李超等,2015)。前两种假说表岩浆成因,第三种假说表岩浆热液成因。

Doroshkevich et al.(2007)提出Pogranichnoe矿床碳酸岩中球粒状石墨不是从C−O−H流体沉淀的,而是从含碳岩浆直接结晶形成的。该学者提出这个观点的主要依据是球粒状石墨充填于硅酸盐矿物间隙,形成类似于海绵陨铁结构。黄羊山矿床中石墨并没有呈现出这种结构,无论是球粒状还是浸染状石墨,石墨都交代硅酸盐矿物,横切矿物边界。此外,有大量热液蚀变矿物绿泥石和绢云母与石墨共生。最主要的,镜下发现主成矿期矿石中与石墨共生的石英内气液两相包裹体含有石墨和黄铜矿子矿物(未发表)。以上三点证据表明主成矿期石墨和硫化物是岩浆热液成因。

Luque et al.(2014)通过测试世界各地石墨矿床碳同位素,得出结论侵入岩赋存的石墨矿床碳质来源通常为地层有机物。黄羊山矿床的第一期和第二期石墨的$\delta^{13}C_{V-PDB}$变化范围分别为−20.5‰~−20.9‰和−20.5‰~−20.7‰,$\Delta\delta^{13}C_{V-PDB}$分别为0.4‰和0.2‰(未发表),表明构成石墨的碳可能来自地层有机物。

据以上结论,将黄羊山矿床球粒状石墨的形成过程总结如下:岩浆在上侵过程中同化混染有机碳质后侵入黄羊山岩体,继而岩浆发生流体不混溶,

分异为球形熔体相和残余熔体相,随着温度和压力的降低,含碳和硫的岩浆热液从球形熔体相中排出并交代熔体,形成大量石墨和硫化物。

6 结 论

(1)矿石岩性为碱长花岗岩,其于晚石炭世((306±4)Ma)后碰撞造山环境中上侵,同化混染地层有机物,碳质从岩浆热液中沉淀形成球粒状石墨,后期又叠加了脉状石墨。其中,前者为主成矿期。

(2)与石墨伴生的金属矿物有磁黄铁矿、黄铜矿、钛铁矿和赤铁矿。这些金属矿物可分为两个世代,第一世代呈自形晶分布于石墨球粒内外,第二世代呈脉状穿插第一世代。

(3)黄羊山石墨矿床碳质来源为地层有机物。

致谢:衷心感谢新疆中材地勘总队在野外工作时给予的诸多关心和帮助;感谢中国科学院广州地球化学研究所的杨毓波研究员在光薄片磨制、锆石挑选、制靶和CL拍照上提供的帮助;感谢中国地质大学(武汉)王露老师在锆石U−Pb定年研究上给予的帮助;感谢审稿老师为本文提出的诸多宝贵意见。

References

Abdallah Nachida, Liegeois Jean − Paul, De Waele Bert, Fezaa Nassima, Ouabadi Aziouz. 2007. The Temaguessine Fe−cordierite orbicular granite (Central Hoggar, Algeria): U−Pb SHRIMP age, petrology, origin and geodynamical consequences for the late Pan−African magmatism of the Tuareg shield[J]. Journal of African Earth Sciences, 49(4/5): 153−178.

Ai Jiang, Lu Xinbiao, Li Zuowu, Wu Yalun. 2018. A super − large graphite deposit discovered in granite rocks at Huangyangshan, Xinjiang, China[J]. China Geology, 1(1): 164−166.

Ballhaus Chris, Fonseca Raul O C, Munker Carsten, Kirchenbaur Maria, Zirner Aurelia. 2015. Spheroidal textures in igneous rocks − Textural consequences of H_2O saturation in basaltic melts[J]. Geochimica et Cosmochimica Acta, 167: 241−252.

Best Myron G. 1982. Igneous and Metamorphic Petrology[M]. San Francisco: W.H. Freeman and Company, 630.

Bi Chengsi, Shen Xiangyuan, Xu Qinsheng, Ming Kuihai, Sun Huili, Zhang Chensheng. 1993. Geological characteristics of stanniferous granites in the Beilekuduk Tin metallogenic belt, Xinjiang[J]. Acta Petrologica et Mineralogica, 12(3): 213− 223(in Chinese with English abstract).

Corfu Fernando, Hanchar John M, Hoskin Paul W O, Kinny Peter. 2003. Atlas of zircon textures[J]. Reviews in Mineralogy and Geochemistry, 53(1): 469−500.

Crespo Elena, Luque Javier, Femandez − Rodriguez Carlos. 2004. Significance of graphite occurrences in the Aracena Metamorphic Belt, Iberian Massif[J]. Geological Magazine, 141(6): 687−697.

Decrite Sylvie, Gasquet Dominique, Marignac Christian. 2002. Genesis of orbicular granitic rocks from the Ploumanac\"h Plutonic Complex (Brittany, France): Petrographical, mineralogical and geochemical constraints[J]. European Journal of Mineralogy, 14(4): 715−731.

Diaz−Alvarado J, Rodriguez N, Rodriguez C, Fernandez C, Constanzo I. 2017. Petrology and geochemistry of the orbicular granitoid of Caldera, northern Chile. Models and hypotheses on the formation of radial orbicular textures[J]. Lithos, 284−285: 327−346.

Doroshkevich A G, Wall F, Ripp G S. 2007. Magmatic graphite in dolomite carbonatite at Pogranichnoe, North Transbaikalia, Russia[J]. Contribution to Mineralogy and Petrology, 153(3): 339−353.

Elliston John N. 1984. Orbicules: an indication of the crystallization of hydrosilicates, Ⅰ[J]. Earth Science Reviews, 20(4): 265−344.

Fernandez C, Castro A. 1999. Brittle behavior of granitic magma: the example of Puente del congosto, Iberian massif, Spain[J]. Geological Society, London, Special Publications, 168(1): 191−206.

Gao Huaizhong, Zhang Wangsheng, Sun Huashan. 2000. A product of plate collision − metallogenic control of highly strained structural belt to Eastern Junggar gold deposit[J]. Geology and Prospecting, 36(3): 15−21(in Chinese with English abstract).

Grosse Pablo, Toselli Alejandro J, Rossi Juana N. 2010. Petrology and geochemistry of the orbicular granitoid of Sierra de Velasco (NW Argentina) and implications for the origin of orbicular rocks[J]. Geological Magzine, 147(3): 451−468.

Hao Ziguo, Fei Hongcai, Hao Qingqing, Liu Lian. 2016. "Three Rare Mineral Resources" and crystalline graphite have become prospecting focuses in China[J]. Acta Geologica Sinica, 90(5): 1905−1906.

Huang Gang, Niu Guangzhi, Wang Xinlu, Guo Jun, Yu Feng. 2017. The discovery of the amphibolite in the Kalamaili ophiolitic mélange formed in mid − oceanic ridge setting[J]. Geology in China, 44(2): 358−370(in Chinese with English abstract).

Huang Gang, Niu Guangzhi, Zhang Zhanwu, Wang Xinlu, Xu Xueyi, Guo Jun, Yu Feng. 2013. Discovery of ~4.0 Ga detrital zircons in the Aermantai ophiolitic mélange, East Junggar, northwest China[J]. Chinese Science Bulletin, 58(30): 3645−3663.

Huizenga J M. 2011. Thermodynamic modeling of a cooling C−O−H fluid − graphite system: implications for hydrothermal graphite precipitation[J]. Mineralium Deposita, 46: 23−33.

Jewell S, Kimball S M. 2017. Mineral Commodity Summaries 2017[R]. U.S. Geological Survey, 201. https://minerals.usgs.gov/minerals/pubs/mcs/2017/mcs2017.pdf

Jiang Gaozhen. 2016. Gold and Graphite Deposits Prospecting in Bayan Obo Rift, Inner Mongolia[D]. Beijing: China University of

Geosciences, 163(in Chinese with English abstract).

Li Chao, Wang Denghong, Zhao Hong, Pei Haoxiang, Li Xinwei, Zhou Limin, Du Andao, Qu Wenjun. 2015. Minerogenetic regularity of graphite deposits in China[J]. Mineral Deposits, 34(6): 1223−1236(in Chinese with English abstract).

Li Jinyi. 2004. Late Neoproterozoic and Paleozoic tectonic framework and evolution of Eastern Xinjiang, NW China[J]. Geological Review, 50(3): 304−322(in Chinese with English abstract).

Li Jinyi, Xiao Xuchang, Tang Yaoqing, Zhao Min, Zhu Baoqing, Feng Yimin. 1990. Main characteristics of Late Paleozoic plate tectonics in the southern part of East Junggar, Xinjiang[J]. Geological Review, 36(4): 305−316(in Chinese with English abstract).

Lin Jinfu, Yu Hengxiang, Yu Xinqi, Di Yongjun, Tian Jiantao. 2007. Zircon SHRIMP U−Pb dating and geological implication of the Sabei alkali−rich granite from Eastern Junggar of Xinjiang, NW China[J]. Acta Petrologica Sinica, 23(8): 1876− 1884(in Chinese with English abstract).

Lindh Anders, Nasstrom Helena. 2006. Crystallization of orbicular rocks exemplified by the Slattemossa occurrence, southeastern Sweden[J]. Geological Magazine, 143(5): 713−722.

Liu Guanghai, Chen Renyi, Bai Daming, Dong Yingjun, Xue Guangqi, Wang Junheng, Xiong Shouqing, Mao Yuyuan. 1995. Metallogenic Features and General Prospecting Approaches on Cu−Au Mines in East Junggar[M]. Beijing: Geological Publishing House, 190(in Chinese).

Liu Jiayuan, Yu Hengxiang, Lin Jinfu. 1998. Two kinds of granitic metallogenetic magmatic formations and their deposit series of East Junggar, Xinjiang[J]. Journal of Guilin Institute of Technology, 18(3): 205−214(in Chinese with English abstract).

Liu Jiayuan, Yu Hengxiang, Wu Guoquan. 1997. Alkali granites and tin deposits of the Kalamiali area, Northern Xinjiang[J]. Geological Exploration for Non−Ferrous Metals, 6(3): 129− 135(in Chinese with English abstract).

Liu Jiayuan, Yu Hengxiang, Wu Guoquan. 1999. Two kinds of alkaline granites in Eastern Junggar, Xinjiang and their geological significance[J]. Bulletin of Mineralogy, Petrology and Geochemistry, 18(2): 89−94(in Chinese with English abstract).

Liu Songbai, Yang Meizhen, Wu Hong'en, Zhao Wenping, Zhang Lianlian. 2011. Metallogenic model of graphite deposit from Sujiquan, Eastern Junggar[J]. Xinjiang Geology, 29(2): 178− 182 (in Chinese with English abstract).

Luque F J, Pasteris Jill D, Wopenka B. 1998. Natural fluid−deposited graphite: Mineralogical characteristics and mechanisms of formation[J]. American Journal of Science, 298(6): 471−498.

Luque F J, Crespo Elena, Barrenechea J F, Ortega L. 2012. Carbon isotopes of graphite: Implications on fluid history[J]. Geoscience Frontiers, 3(2): 197−207.

Luque F J, Huizenga J − M, Crespo − Feo E, Wada H, Ortega L, Barrenechea J F. 2014. Vein grahite deposits: Geological settings, origin, and economic significance[J]. Mineralium Deposita, 49(2): 261−277.

Meyer H P, Alther R. 1991. A model for the genesis of orbicular granitoid rocks[J]. Terra Abstracts, 3: 426.

Mo Rujue, Liu Shaobing, Huang Cuirong, Zhang Guangrong, Tan Guanmin, Wang Baoxian, Xiao Xiangzhang. 1989. Geology of Graphite Deposits in China[M]. Beijing: China Architecture and Building Press, 290(in Chinese).

Neef G. 1991. Rod − like and orbicular structure in mid Devonian feldspar porphyries, New South Wales, Australia[J]. Lithos, 27(3): 205−212.

Nie Feng, Tian Xiaoli, Li Zhensheng. 2014. Age and provenance of the original Devonian in the eastern Junggar orogenic belt: The evidence of detrital zircon U − Pb geochronology[J]. Chinese Journal of Geology, 49(2): 695− 717(in Chinese with English abstract).

Nie Xiaoyong, Liu Jiajun, Su Dayong, Zhang Xiangyun. 2016. Zircon U−Pb age of the east Qingshui plagiogranite in Kalamaili belt of Xinjiang and its geological implications[J]. Geology in China, (5): 1729−1736(in Chinese with English abstract).

Ortega L, Millward D, Luque F J, Barrenechea J F, Beyssac O, Huizenga J M, Rodas M, Clarke S M. 2010. The graphite deposit at Borrowdale (UK): A catastrophic mineralizing event associated with Ordovician magmatism[J]. Geochimica Cosmochimica Acta, 74(8): 2429−2449.

Qin Xueqing, Liu Yuanzhen. 1986. Discussion on the genesis of Sujiquan graphite deposit in Xinjiang[J]. Building Materials Geology, 2: 13−17(in Chinese with English abstract).

Rosing−Schow Nanna, Bagas Leon, Kolb Jochen, Balic−Zunic Tonci, Korte Christoph, Fiorentini Marco L. 2017. Hydrothermal flake graphite mineralization in Paleoproterozoic rocks of south − east Greenland[J]. Mineralium Deposita, 52(5): 769−789.

Rumble D. 2014. Hydrothermal graphitic carbon[J]. Elements, 10(6): 427−433.

Sen Yuanwang, Chuan Xiuyun, Bao Ying, Wei ChunJing. 2012. Orbicular graphite from Oshirabetsu, Hokkaido, Japan[J]. Bulletin of Mineralogy, Petrology and Geochemistry, 26: 143− 144(in Chinese with English abstract).

Smillie Robert W, Turbull Rose E. 2014. Field and petrographical insight into the formation of orbicular granitoids from the Bonney Pluton, southern Vectoria Land, Antarctica[J]. Geological Magazine, 151(2): 534−549.

Song Lihong, Zhu Guang, Gu Chengchuan, Zhai Mingjian. 2015. Orogeny − related activities of Kalamaili fault zone and their indications to the orogenic processes[J]. Geological Review, 61(1): 79−94(in Chinese with English abstract).

Su Yuping, Tang Hongfeng, Liu Congqiang, Hou Guangshun, Liang Lili. 2006. The determination and a preliminary study of Sujiquan aluminous A − type granites in East Junggar, Xinjiang[J]. Acta

Petrologica et Mineralogica, 25(3): 175− 184(in Chinese with English abstract).

Taylor R P, Ikingura J R, Fallick A E, Huang Y, Watkinson D H. 1992. Stable isotope compositions of tourmalines from granites and related hydrothermal rocks of the Karagwe − Ankolean Belt, Northwest Tanzanian[J]. Chemical Geology, 94: 215−227.

Tang Hongfeng, Qu Wenjun, Su Yuping, Hou Guangshun, Du Andao, Cong Feng. 2007. Genetic connection of Sareshike tin deposit with the alkaline A−type granites of Sabei body in Xinjiang: constraint from isotopic ages[J]. Acta Petrologica Sinica, 23(8): 1989− 1997 (in Chinese with English abstract).

Tang Yanling, Mei Houjun, Pan Keyue, Liu Dequan, Zhou Ruhong, Xin Hongguang. 2005. Non − metallic Ore Deposits in Xinjiang, China[M]. Beijing: Geological Publishing House, 313(in Chinese).

Vernon Ron H. 1985. Possible role of superheated magma in the formation of orbicular granitoids[J]. Geology, 13(12): 843−845.

Wang Jingbing, Xu Xin. 2006. Post−collisional tectonic evolution and metallogenensis in northern Xinjiang, China[J]. Acta Geologica Sinica, 80(1): 23−31(in Chinese with English abstract).

Wu Guoquan, Liu Jiayuan, Yuan Kuirong. 1997. The composition of the Kelameili high − alkaline granite belt, Xinjiang[J]. Journal of Guilin Institute of Technology, 17(1): 18− 25(in Chinese with English abstract).

Xiao Wenjiao, Windley B F, Yan Quanren, Qin Kezhang, Chen Hanlin, Yuan Chao, Sun Min, Li Jiliang, Sun Shu. 2006. SHRIMP Zircon age of the Aermantai ophiolite in the North Xinjiang area, China and its tectonic implications[J]. Acta Geologica Sinica, 80(1): 32−37(in Chinese with English abstract).

Yan Zhengfu, Yang Hao, Gu Lianxing, Guo Jichun. 1990. Geology and genesis of the Sujiquan Graphite deposit, Xinjiang[J]. Jiangsu Geology, (3): 21−24(in Chinese with English abstract).

Yang Baokai, Li Yongjun, Wu Hong'en, Yan Jing, Tian Zhixian, Liu Zhenwei, Wang Yabing. 2010. Discussion on genesis of graphite deposits in Sujiquan area, Kalamely, East Junggar[J]. Journal of Earth Sciences and Environment, 32: 194−195(in Chinese).

Yang Gaoxue, Li Yongjun, Si Guohui, Wu Hong'en, Zhang Yongzhi, Jing Zhao. 2009a. Petrological characteristic of the Huangyangshan intrusion in Kalamaili area, East Junggar, Xinjiang[J]. Journal of Earth Sciences and Environment, 31(1): 34− 41(in Chinese with English abstract).

Yang Gaoxue, Li Yongjun, Wu Hong'en, Si Guohui, Jin Zhao, Zhang Yongzhi. 2009b. LA − ICP − MS zircon U − Pb dating of the Huangyangshan pluton and its enclaves from Kalamaili area eastern Junggar, Xinjiang, and geological implications[J]. Acta Petrologica Sinica, 25(12): 3197− 3207(in Chinese with English abstract).

Yang Gaoxue, Li Yongjun, Wu Hong'en, Si Guohui, Zhang Yongzhi, Jin Zhao. 2010. A tentative discussion on the genesis of Huangyangshan granite body in Kalamaili orogen, East Junggar[J]. Acta Geoscientica Sinica, 31(2): 170−182(in Chinese with English abstract).

Yang Gaoxue, Li Yongjun, Wu Hong'en, Zhong Xing, Yang Baokai, Yan Cunxing, Yan Jing, Si Guohui. 2011. Geochronological and geochemical constrains on petrogenesis of the Huangyangshan A−type granite from the East Junggar, Xinjiang, NW China[J]. Journal of Asian Earth Sciences, 40: 722−736.

Yu Hengxiang, Wu Guoquan, Liu Jiayuan. 1998. The two ore−forming metals series closely related to the two granitoid series in Eastern Junggar, Xinjiang[J]. Geotectonica et Metallogenia, 22(2): 119−127 (in Chinese with English abstract).

Zhang Dong, Lu Yanming, Fan Junjie, Pan Aijun, Zhang Yujie, Chao Yinyin. 2011. Two types of granitoid rocks in the northern margin of the Eastern Junggar area and their geological implications[J]. Geology and Exploration, 47(4): 577−592(in Chinese with English abstract).

Zhang Guoxin, Hu Aiqin, Zhang Hongbin, Zhang Qianfeng, Shen Youlin. 1996. Carbon isotopic evidence for the origin of the spherical graphite in a granite−hosted graphite deposit, Sujiquan, Xinjiang, China[J]. Geochimica, 25(4): 379− 386(in Chinese with English abstract).

Zhang Xiaolin, Fan Wenjun, Li Zuowo, Chen Zhengguo, Chen Junyuan. 2017. The discovery of a superlarge magmatic graphite deposit in Huangyangshan area, Qitai Country, Xinjiang[J]. Geology in China, 44(5): 1033−1034(in Chinese).

Zhang Yujie, Zhang Dong, Lu Yanming, Fan Junjie, Pan Aijun, Zhang Feng. 2013. Multi − stage tectonic deformation and superimposed gold mineralization in the Karamaili structural belt of Eastern Junggar, Xinjiang[J]. Geology and Exploration, 49(5): 797−812(in Chinese with English abstract).

Zhao Lei, Niu Baogui, Xu Qinqin, Yang Yaqi. 2019. An analysis of Silurian − Carboniferous sedimentary and structural characteristics on both sides of Karamaili ophiolitic belt of Xinjiang and its significance[J]. Geology in China, 46(3): 615−628(in Chinese with English abstract).

Zuilen Mark A, Lepland Aivo, Teranes Jane, Finarelli John, Wahlen Martin, Arrhenius Gustaf. 2003. Graphite and carbonates in the 3.8 Ga old Isua Supracrustal Belt, southern West Greenland[J]. Precambrian Research, 126(3): 331−348.

Zurevinski Shannon E, Mitchell Roger H. 2015. Petrogenesis of orbicular ijolites from the Prairie Lake complex, Marathon, Ontario: Textural evidence from rare processes of carbonatitic magmatism[J]. Lithos, 239: 234−244.

附中文参考文献

毕承思,沈湘元,徐庆生,明奎海,孙惠礼,张春生. 1993. 新疆贝勒库都克锡矿带含锡花岗岩地质特征[J]. 岩石矿物学杂志,12(3): 213−223.

高怀忠,张旺生,孙华山. 2000. 板块碰撞产物——强应变构造带对

东准噶尔金矿的控制[J]. 地质与勘探,36(3): 15−21.

黄岗,牛广智,王新录,郭俊,宇峰. 2017. 东准噶尔卡拉麦里蛇绿混杂岩中斜长角闪岩的发现与洋中脊构造环境的确认[J]. 中国地质,44(2): 358−370.

姜高珍. 2016. 内蒙古白云鄂博裂谷系金矿石墨矿成矿预测综合研究[D]. 北京:中国地质大学,163.

李超,王登红,赵鸿,裴浩翔,李欣尉,周利敏,杜安道,屈文俊. 2015. 中国石墨矿床成矿规律概要[J]. 矿床地质,34(6): 1223−1236.

李锦轶. 2004. 新疆东部新元古代晚期和古生代构造格局及其演变[J]. 地质论评,50(3): 304−322.

李锦轶,肖序常,汤耀庆,赵民,朱宝清,冯益民. 1990. 新疆东准噶尔卡拉麦里地区晚石生代板块构造的基本特征[J]. 地质论评,36(4): 305−316.

林锦富,喻亨祥,余心起,狄永军,田建涛. 2007. 新疆东准噶尔萨北富碱花岗岩SHRIMP锆石U−Pb测年及其地质意义[J]. 岩石学报,23(8): 1876−1884.

刘光海,陈仁义,白大明,董英君,薛光琦,王君恒,熊寿庆,毛玉元. 1995. 东准噶尔铜金矿成矿特征及综合评价方法[M]. 北京:地质出版社,149.

刘家远,喻亨祥,林锦富. 1998. 新疆东准噶尔两类花岗质成矿岩浆建造及其矿床系列[J]. 桂林工学院学报,18(3): 205−214.

刘家远,喻亨祥,吴郭泉. 1997. 新疆北部卡拉麦里富碱花岗岩带的碱性花岗岩与锡矿[J]. 有色金属矿产与勘查,6(3): 129−135.

刘家远,喻亨祥,吴郭泉. 1999. 新疆东准噶尔两类碱性花岗岩及其地质意义[J]. 矿物岩石地球化学通报,18(2): 89−94.

刘松柏,杨梅珍,吴洪恩,赵文平,张练练. 2011. 新疆苏吉泉球状石墨矿床成矿模式[J]. 新疆地质,29(2): 178−182.

莫如爵,刘绍斌,黄翠蓉,张光荣,谭冠民,王宝娴,肖祥章. 1989. 中国石墨矿床地质[M]. 北京:中国建筑工业出版社,290.

聂峰,田晓丽,李振生. 2014. 东准造山带原泥盆系的形成时代及源区:碎屑锆石U−Pb年代学证据[J]. 地质科学,49(2): 695−717.

聂晓勇,刘家军,苏大勇,章享云. 2016. 新疆卡拉麦里清水东斜长花岗岩的锆石U−Pb年龄及地质意义[J]. 中国地质,(5): 1729−1736.

秦学庆,刘远珍. 1986. 新疆苏吉泉石墨矿床成因探讨[J]. 建材地质,2: 13−17.

森原望,传秀云,鲍莹,魏春景. 2012. 日本北海道音调津的球状石墨[J]. 矿物岩石地球化学通报,26: 143−144.

宋利宏,朱光,顾承串,翟明见. 2015. 卡拉麦里断裂带造山期活动规律及其对造山过程的指示[J]. 地质论评,61(1): 79−94.

苏玉平,唐红峰,刘丛强,侯广顺,梁莉莉. 2006. 新疆东准噶尔苏吉泉铝质A型花岗岩的确立及其初步研究[J]. 岩石矿物学杂志,25(3): 175−184.

唐红峰,屈文俊,苏玉平,侯广顺,杜安道,丛峰. 2007. 新疆萨惹什克锡矿与萨北碱性A型花岗岩成因关系的年代学制约[J]. 岩石学报,23(8): 1989−1997.

唐延龄,梅厚钧,潘克跃,刘德权,周汝洪,辛恒广. 2005. 中国新疆非金属矿床[M]. 北京:地质出版社,313.

王京彬,徐新. 2006. 新疆北部后碰撞构造演化与成矿[J]. 地质学报,80(1): 23−31.

吴郭泉,刘家远,袁奎荣. 1997. 新疆卡拉麦里富碱花岗岩带组成[J]. 桂林工学院学报,17(1): 18−25.

肖文交,B F Windley,阎全人,秦克章,陈汉林,袁超,孙敏,李继亮,孙枢. 2006. 北疆地区阿尔曼太蛇绿岩锆石SHRIMP年龄及其大地构造意义[J]. 地质学报,80(1): 32−37.

严正富,杨浩,顾连兴,郭继春. 1990. 新疆苏吉泉石墨矿床地质特征及其成因[J]. 江苏地质,(3): 21−24.

杨宝凯,李永军,吴宏恩,严镜,田陟贤,刘振伟,汪雅兵. 2010. 东准卡拉麦里地区苏吉泉一带石墨矿床成因探讨[J]. 地球科学与环境学报,32: 194−195.

杨高学,李永军,司国辉,吴宏恩,张永智,金朝. 2009a. 东准噶尔卡拉麦里地区黄羊山岩体岩石学特征[J]. 地球科学与环境学报,31(1): 34−41.

杨高学,李永军,吴宏恩,司国辉,金朝,张永智. 2009b. 东准噶尔卡拉麦里地区黄羊山花岗岩和包体LA−ICP−MS锆石U−Pb测年及地质意义[J]. 岩石学报, 25(12): 3197−3207.

杨高学,李永军,吴宏恩,司国辉,张永智,金朝. 2010. 东准噶尔卡拉麦里黄羊山花岗岩岩石成因探讨[J]. 地球学报,31(2): 170−182.

喻亨祥,吴郭泉,刘家远. 1998. 新疆东准噶尔地区两类花岗岩与两个成矿系列[J]. 大地构造成矿学,22(2): 119−127.

张栋,路彦明,范俊杰,潘爱军,张玉杰,朝银银. 2011. 东准噶尔北缘两类花岗质岩石及其地质意义[J]. 地质与勘探,47(4): 577−592.

张国新,胡霭琴,张鸿斌,张前锋,申佑林. 1996. 新疆苏吉泉石墨矿床成因的碳同位素证据[J]. 地球化学,25(4): 379−386.

张小林,樊文军,李作武,陈正国,陈军元. 2017. 新疆奇台县黄羊山发现超大型晶质石墨矿床[J]. 中国地质,44(5): 1033−1034.

张玉杰,张栋,路彦明,范俊杰,潘爱军,张峰. 2013. 新疆东准噶尔卡拉麦里构造带多期变形和金叠加成矿[J]. 地质与勘探,49(5): 797−812.

赵磊,牛宝贵,徐芹芹,杨亚琦. 2019. 新疆东准噶尔卡拉麦里蛇绿岩带两侧志留系—石炭系沉积和构造特征分析及其意义[J]. 中国地质,46(3): 615−628.